J|A|C|S COMMUNICATIONS

Published on Web 04/17/2009

Side Chain Resonances in Static Oriented Proton-Decoupled ^{15}N Solid-State NMR Spectra of Membrane Proteins

Christopher Aisenbrey,[†,‡] Lydia Prongidi-Fix,[†] Alexandre Chenal,[§] Daniel Gillet,[||] and Burkhard Bechinger*[,†,‡]

Insitut de Chimie, Université de Strasbourg, CNRS UMR7177, 4 rue Blaise Pascal, 67070 Strasbourg, France, Max-Planck-Institut für Biochemie, Am Klopferspitz 18a, 82152 Martinsried, Germany, Institut Pasteur, CNRS URA 2185, Unité de Biochimie des Interactions Macromoléculaires, Département de Biologie Structurale et Chimie, 25-28 rue du Dr Roux, 75724 Paris cedex 15, France, and CEA, iBiTecS, SIMOPRO, Gif sur Yvette, F-91191, France

Received January 28, 2009; E-mail: bechinger@chimie.u-strasbg.fr

Solid-state NMR spectroscopy is a powerful technique to investigate the structure, topology, and dynamics of proteins in microcrystals[1−4] or when reconstituted into membranes.[5−11] On the one hand magic angle spinning multidimensional high-resolution solid-state NMR spectra are obtained from proteins labeled with ^{15}N and ^{13}C provided that the sample is characterized by a high local order. The correlations that are detected in these spectra provide valuable distance and chemical shift information that can be used for structural analysis. On the other hand, in static oriented samples the orientation-dependent NMR parameters such as chemical shift, dipolar coupling, or quadrupolar splitting provide the angular constraints that are required for the analysis of the structure, dynamics, and topology of polypeptides. Many experiments have been performed on peptides carrying specific labels but also on proteins, which have been overexpressed in bacteria and labeled with ^{15}N uniformly or selectively.[7−9,12−15] As the anisotropy of the amide resonances covers the range from 50 to 230 ppm, there is considerable overlap with ^{15}N side chain resonances, most of which exhibit isotropic peak positions in the same ^{15}N chemical shift range.[16] Although the resonances of mobile sites are much attenuated by using the cross-polarization techniques, these resonances have been observed in many NMR spectra and hamper the assignment as well as the structural and topological analysis of spectra obtained from these oriented samples, a key issue which has so far attracted little attention.

Figure 1A shows the proton-decoupled ^{15}N solid-state NMR spectrum of purple membranes of *Halibacterium salinarum*, labeled uniformly with ^{15}N [17] and oriented with their normal parallel to the magnetic field direction. The composition of this two-dimensional crystal array is dominated by the only protein component, i.e., the light-driven proton pump bacteriorhodopsin (bR). The structures of this 26 kD protein are characterized by seven transmembrane helices, and the conformational changes during the photocycle have been extensively analyzed by X-ray crystallography and electron microscopy.[18,19] When the ^{15}N spectrum of dark adapted bR is compared to the simulated spectrum arising from the backbone amide nitrogens of this protein, it becomes obvious that the first exhibits considerable additional intensities <130 ppm (Figure 1A, B). These could arise from nonoriented membranes as well as from side chains, as the isotropic chemical shift positions of lysine (37 ppm), arginine (74 ppm and 88 ppm), tryptophane (84 ppm), asparagine and glutamine (118 ppm) all occur in the spectral region shown at positions that are indicated by the simulation also represented in Figure 1B.[16,20] In addition the isotropic histidine side chains resonate in the range 170/178 ppm (cationic side chain) and around 170/245 ppm (uncharged),[16] but in the case of bR this amino acid is absent.[21]

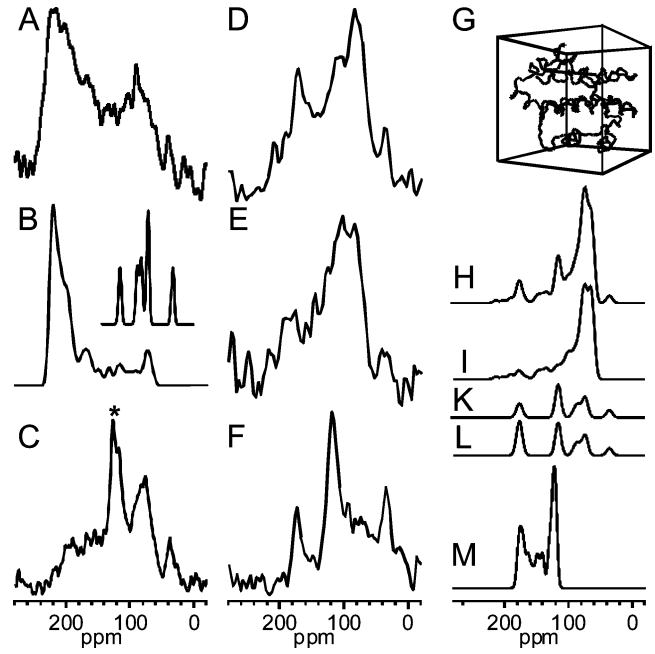

Figure 1. Proton-decoupled ^{15}N solid-state NMR spectra of uniformly labeled proteins, reconstituted into phospholipid membranes oriented with their normal parallel to the magnetic field direction. Experimental spectra of 2 mg of purple membranes at 93% r.h. are shown in panels A and C, whereas the simulated spectrum of the bR backbone (bottom) and side chain resonances (top) are shown in panel B. D, E and F show ^{15}N spectra of 2.5 mg of diphtheria toxin T domain reconstituted into 100 mg of oriented POPC/POPG 4:1 membranes at pH 4 and equilibrated at 93% r.h. (D) or 100% r.h (E,F). The spectra were recorded by cross-polarization (A,D,E), or using a Hahn-echo sequence (C,F). Simulated spectra of the backbone and side chain resonances of Bcl-x_L (ΔC) uniformly labeled with ^{15}N at an alignment (G) that represents reasonably well the experimental spectra of ref 14 are shown to illustrate the contributions of the backbone and side chains (H), the backbone alone (I), the side chains (K), and the side chains including a 6 histidine tag (L). The simulated spectral intensities from the backbone of a uniformly ^{15}N labeled helix tilted at 45° are shown in M. The ^{15}N cross-polarization NMR experiments were recorded analogous to ref 14 and the spectra referenced relative to NH_4Cl (41.5 ppm). The simulations were performed following the indications of ref 22 using the PDB data files 2AT9 and 1MAZ, respectively.

It should be noted that the simulation of the contributions of the side chains (or mobile amide residues with isotropic chemical shifts

[†] Université de Strasbourg.
[‡] Max-Planck-Institut für Biochemie.
[§] Institut Pasteur.
[||] CEA.

10.1021/ja900677b CCC: $40.75

of ~110−120 ppm)[23] is hampered by the fact that mobile sites do not cross-polarize with the same efficiency and relaxation behavior as static amide backbone resonances. Therefore, in cross-polarization experiments the intensity of mobile amide or side chain residues is much reduced when compared to the backbone. To complicate matters the cross-polarization efficiency depends on the motions of each individual side chain in a differential manner as well as the detailed experimental conditions such as temperature, hydration, cross-polarization method, or contact time.[24,25] Furthermore the line width and anisotropy of the side chain resonances also depend on the sample preparation. This can in part explain the subtle differences in line shapes when labeled purple membranes have been investigated by different authors (Figure 1A,C and refs 8 and 9). However, when the same sample is analyzed by a proton-decoupled 90 °−τ−180 °−τ-acqusition pulse sequence (Hahn echo) isotropic resonances of the purple membrane are clearly visible with maxima at 118, 82, and 37 ppm and dominate the spectrum (Figure 1C). Mobile amide sites, including the most N-terminal and about 20 C-terminal residues of bR, not giving well-defined electron densities in crystallographic analyses,[18,19] contribute to the peak at 126 ppm (labeled with a star).

In a next series of experiments the 20 KDa translocation (T) domain of the diphtheria toxin of *Corynebacterium diphtheriae* was investigated. The pH-dependent membrane insertion of the T domain mediates the translocation of the catalytic domain of the toxin into the cytosol of targeted cells. The protein was uniformly labeled with ^{15}N[26] and reconstituted into oriented POPC/POPG 4:1 phospholipid bilayers at pH 4. When the sample is equilibrated at 93% r.h., relatively sharp spectral intensities are obvious at 36 and 171 ppm (Figure 1D). These intensities are less apparent in the cross-polarization solid-state NMR spectrum recorded at 100% r.h. (Figure 1E) but predominate when a spectrum is recorded of the fully hydrated sample using a Hahn-echo pulse sequence where maxima are observed at 34, 119, and 173 ppm (Figure 1F). It is also obvious from the comparison of Figure 1E and F that the Hahn-echo pulse sequence is much less sensitive when compared to the cross-polarization sequence when immobile sites are concerned. Purification of this protein was performed by His-tag affinity chromatography, and the signal intensities of 6 additional histidines contribute to the spectrum (14 His in total). Notably, the side chain intensities at 171 ppm are very visible at the lower hydration where the mobility of the protein is probably hindered by the close stacking of phospholipid bilayers which leaves less space for large amplitude motions.

As a last example the spectral modifications by the side chain resonances are illustrated by a simulation of the spectrum of Bcl-x_L, truncated of its C-terminus (ΔC), when being associated with oriented lipid membranes at alignments of the membrane normal parallel to the magnetic field direction. This antiapoptotic protein encompasses 209 residues and is an important regulator of controlled cell death. Previously, some ambiguity, related to residual side chain signal intensities, arose as to the interpretation of the experimental ^{15}N solid-state NMR spectra of this protein after reconstitution into oriented membranes.[13,14] We therefore simulated the spectra arising from the backbone (Figure 1I), the side chains (Figure 1K,L), or the backbone and side chain nitrogens (Figure 1H) at an alignment of the protein relative to the membrane normal that represents reasonably well the experimental spectra obtained in a previous investigation.[14] The data are indicative of Bcl-x_L being a type I membrane protein where most of the helical domains of this 20 kDa protein are predominantly oriented parallel to the membrane surface (Figure 1G).[14] Furthermore, comparison of Figure 1H, L, and M illustrate the coincidence of histidine and other isotropic mobile resonances with the maxima that are obtained from a 45° tilted helix.[22] Therefore, the histidine side chain intensities could be confounded with helical domains that are oriented at tilt angles of ~45°, in particular when additional isotropic intensities are simultaneously present in the 110−120 ppm range (isotropic Asn, Gln and amides). However, the isotropic signal intensities can be identified by comparing the solid-state NMR spectra obtained by cross-polarization with a spectrum obtained by a Hahn-echo pulse sequence. Whereas the former shows only residual intensities of mobile residues (Figure 1D,E), the Hahn-echo sequence is more quantitative in their representation, although overall this latter approach is also much less sensitive (Figure 1F). Furthermore, the appearance of mobile lysine side chains which resonate outside the chemical shift range of the backbone amides can be taken as an indication that under the experimental conditions other mobile side chain resonances probably also contribute to the spectra.

Acknowledgment. We are thankful to Brigitte Kessler and Dieter Oesterhelt for the kind gift of ^{15}N labeled purple membranes. The financial support by the ANR, VLM, the EU (MCRTN-33439), and ARC is gratefully acknowledged.

Supporting Information Available: Complete ref 23 and a more detailed discussion of Figure 1. This material is available free of charge via the Internet at http://pubs.acs.org.

References

(1) Lange, A.; Becker, S.; Seidel, K.; Giller, K.; Pongs, O.; Baldus, M. *Angew. Chem., Int. Ed.* **2005**, *44*, 2089–2092.
(2) Bockmann, A. *Magn. Reson. Chem.* **2007**, *45*, S24−S31.
(3) Castellani, F.; van Rossum, B.; Diehl, A.; Schubert, M.; Rehbein, K.; Oschkinat, H. *Nature (London)* **2002**, *420*, 98–102.
(4) Frericks, H. L.; Zhou, D. H.; Yap, L. L.; Gennis, R. B.; Rienstra, C. M. *J. Biomol. NMR* **2006**, *36*, 55–71.
(5) Bechinger, B.; Sizun, C. *Concepts Magn. Reson.* **2003**, *18A*, 130–145.
(6) Davis, J. H.; Auger, M. *Prog. NMR Spectrosc.* **1999**, *35*, 1–84.
(7) Tian, C.; Gao, P. F.; Pinto, L. H.; Lamb, R. A.; Cross, T. A. *Protein Sci.* **2003**, *12*, 2597–2605.
(8) Kamihira, M.; Vosegaard, T.; Mason, A. J.; Straus, S. K.; Nielsen, N. C.; Watts, A. *J. Struct. Biol.* **2005**, *149*, 7–16.
(9) Soubias, O.; Reat, V.; Saurel, O.; Milon, A. *Magn. Reson. Chem.* **2004**, *42*, 212–217.
(10) Lange, A.; Giller, K.; Hornig, S.; Martin-Eauclaire, M. F.; Pongs, O.; Becker, S.; Baldus, M. *Nature (London)* **2006**, *440*, 959–962.
(11) Andronesi, O. C.; Becker, S.; Seidel, K.; Heise, H.; Young, H. S.; Baldus, M. *J. Am. Chem. Soc.* **2005**, *127*, 12965–12974.
(12) Opella, S. J.; Zeri, A. C.; Park, S. H. *Annu. Rev. Phys. Chem.* **2008**, *59*, 635–657.
(13) Franzin, C. M.; Choi, J.; Zhai, D.; Reed, J. C.; Marassi, F. M. *Magn. Reson. Chem.* **2004**, *42*, 172–179.
(14) Aisenbrey, C.; Sudheendra, U. S.; Ridley, H.; Bertani, P.; Marquette, A.; Nedelkina, S.; Lakey, J. H.; Bechinger, B. *Eur. Biophys. J.* **2007**, *36*, 451–460.
(15) Aisenbrey, C.; Cusan, M.; Lambotte, S.; Jasperse, P.; Georgescu, J.; Harzer, U.; Bechinger, B. *ChemBioChem.* **2008**, *9*, 944–951.
(16) Witanowski, M.; Stefanik, L.; Webb, G. A. *Annu. Rep. NMR Spectrosc.* **1986**, *18*, 2.
(17) Patzelt, H.; Ulrich, A. S.; Egbringhoff, H.; Dux, P.; Ashurst, J.; Simon, B.; Oschkinat, H.; Oesterhelt, D. *J. Biomol. NMR* **1997**, *10*, 95–106.
(18) Haupts, U.; Tittor, J.; Oesterhelt, D. *Annu. Rev. Biophys. Biomol.* **1999**, *28*, 367–399.
(19) Heberle, J.; Fitter, J.; Sass, H. J.; Buldt, G. *Biophys. Chem.* **2000**, *85*, 229–248.
(20) Lambotte, S.; Jasperse, P.; Bechinger, B. *Biochemistry* **1998**, *37*, 16–22.
(21) Khorana, H. G.; Gerber, G. E.; Herlihy, W. C.; Gray, C. P.; Anderegg, R. J.; Nihei, K.; Biemann, K. *Proc. Natl. Acad. Sci. U.S.A.* **1979**, *76*, 5046–5050.
(22) Bechinger, B.; Aisenbrey, C.; Bertani, P. *Biochim. Biophys. Acta* **2004**, *1666*, 190–204.
(23) Eldon, L. U.; et al. *Nucleic Acids Res.* **2007**, *36*, D402–D408 (doi: 10.1093/nar/gkm957).
(24) Aisenbrey, C.; Bechinger, B. *J. Am. Chem. Soc.* **2004**, *126*, 16676–16683.
(25) Prongidi-Fix, L.; Bertani, P.; Bechinger, B. *J. Am. Chem. Soc.* **2007**, *129*, 8430–8431.
(26) Chenal, A.; Prongidi-Fix, L.; Perier, A.; Vernier, G.; Lambotte, S.; Fragneto, G.; Bechinger, B.; Gillet, D.; Forge, V.; Ferrand, M. Submitted.

JA900677B